

1  
2  
3  
4  
5  
6  
7  
8  
9  
10  
11  
12  
13  
14  
15  
16  
17  
18  
19  
20  
21  
22  
23

Decolouration of H<sub>2</sub>SO<sub>4</sub> leachate from phosphorus-saturated  
alum sludge using H<sub>2</sub>O<sub>2</sub> and advanced oxidation processes in  
phosphorus recovery strategy

X.H. ZHAO and Y.Q. ZHAO\*

Centre for Water Resources Research, School of Architecture, Landscape and Civil Engineering,  
Newstead Building, University College Dublin, Belfield, Dublin 4, Ireland

---

\*Corresponding author: Tel: +353-1-7163215, Fax: +353-1-7163297  
E-mail: yaqian.zhao@ucd.ie

24 **ABSTRACT**

25 As a part of attempt for phosphorus (P) recovery from P-saturated alum sludge, which was  
26 used as a low-cost P-adsorbent in treatment reed bed for wastewater treatment, decolouration  
27 of H<sub>2</sub>SO<sub>4</sub> leachate obtained from previous experiment, possessing a great deal of P, aluminum  
28 and red-brown coloured materials (RBCMs), by using H<sub>2</sub>O<sub>2</sub> and advanced oxidation processes  
29 (AOPs) was investigated. The use of H<sub>2</sub>O<sub>2</sub> and AOPs in the forms of Fenton (H<sub>2</sub>O<sub>2</sub>/Fe<sup>2+</sup>) and  
30 photo-Fenton (UV/H<sub>2</sub>O<sub>2</sub>/Fe<sup>2+</sup>) were tested. The changes in colour and total organic carbon  
31 (TOC) were taken place as a result of mineralization of RBCMs. The results revealed that all of  
32 these three processes examined were efficient. It was found that about 98 % colour and 47 %  
33 TOC can be removed under photo-Fenton treatment after 8 hours of UV irradiation.  
34 Correspondingly, the reaction rates of H<sub>2</sub>O<sub>2</sub> and Fenton systems were slow, but 100 % colour  
35 and 59 % TOC removal of H<sub>2</sub>O<sub>2</sub> process and 100 % colour and 67 % TOC reductions of  
36 Fenton process can be achieved after 72 hours of reaction. The changes of structure and  
37 molecular weight/size of RBCMs were also evaluated by HPLC and UV-vis spectroscopic  
38 analysis. From the results, some chromophores of RBCMs such as aromatic groups were  
39 appeared to be easily degraded to the smaller refractory components. Hence, based on the  
40 experimental results and considering the investment and expediency of operation, H<sub>2</sub>O<sub>2</sub> and  
41 Fenton oxidation could be suitable technologies for the treatment of the RBCMs derived from  
42 P-extraction stage by using H<sub>2</sub>SO<sub>4</sub> leaching.

43

44 **Keywords:** Natural organic matter; peroxide; advanced oxidation process; Fenton reaction;

45 colour; total organic carbon

46

47

48

## 49 **Introduction**

50

51 During the series of incessant succession of research projects at University College Dublin,  
52 Ireland aimed at investigating the beneficial reuse of a widely generated water industrial by-  
53 product, i.e. dewatered aluminium-coagulated drinking water treatment sludge, as a substrate in  
54 engineered wetlands for wastewater treatment,<sup>[1]</sup> the alum sludge-based engineered wetland  
55 systems have been developed particularly for enhanced phosphorus (P) removal. Such the  
56 development makes a new and novel way of (re)using the waste sludge as opposed to  
57 landfilling it.<sup>[2]</sup> In line with the P recovery study from the P-saturated sludge after use in the  
58 engineered wetlands, P desorption/extraction was investigated and the H<sub>2</sub>SO<sub>4</sub> has been  
59 demonstrated as an efficient and cost-effective reagent for such kind of P extraction.<sup>[3]</sup>  
60 However, soluble organics including some humic substances in the sludge have also been  
61 found to be released to the H<sub>2</sub>SO<sub>4</sub> solution during P extraction since the chemical oxygen  
62 demand (COD) and total organic carbon (TOC) are extremely high in the P extraction solution,  
63 exhibiting a red-brown colour. Thus, the released soluble organics is termed as “red-brown  
64 coloured materials” (RBCMs) in this paper. It is understood that the RBCMs were natural  
65 organic matter (NOM) derived from the source water and transferred to the sludge during the  
66 water purification processes such as coagulation, flocculation, sedimentation and filtration.  
67 Although the RBCMs may contain different kinds of organics, their dark colour is consistent  
68 with some humic substances, which are ubiquitous, heterogeneous biopolymers resulting from  
69 microbial and chemical transformations of organic debris and widely present in terrestrial and  
70 aqueous environments.<sup>[4-6]</sup> Without a doubt, certainly, such the RBCMs have to be removed in  
71 the P recovery process if the pure phosphorus compound is expected to be formed in the P  
72 recovery strategy.

73 Extensive research has been conducted worldwide for the removal of natural organic matters  
74 (NOM) from natural source water. The removal methods include enhanced coagulation,<sup>[7]</sup>  
75 membrane separation,<sup>[8]</sup> carbon adsorption<sup>[9]</sup> and advanced oxidation processes (AOPs).<sup>[10-13]</sup>  
76 AOPs have been emerged as the highly efficient methods for the decomposition of a wide  
77 range of pollutants since they are characterized by generation of very reactive hydroxyl radicals  
78 (HO•), with a non-selective and higher oxidation potential (2.8 V) than that of O<sub>3</sub> (2.07 V),  
79 H<sub>2</sub>O<sub>2</sub> (1.78 V), MnO<sub>4</sub><sup>-</sup> (1.69 V).<sup>[14-16]</sup> In addition, AOPs have been proven to oxidize NOM into  
80 innocuous end products such as CO<sub>2</sub> and H<sub>2</sub>O, without producing other aqueous pollution  
81 problems. Therefore, AOPs are the cutting-edge technologies, which are increasingly adopted  
82 for the removal of many kinds of organic pollutants to meet the new challenges of water  
83 pollution control accompanied with the world economical and societal development.<sup>[17-21]</sup>

84 The objective of this study was to determine the feasibility and effectiveness of using single  
85 oxidants, i.e. H<sub>2</sub>O<sub>2</sub>, and the AOPs of Fenton (H<sub>2</sub>O<sub>2</sub>/Fe<sup>2+</sup>) and Fenton/UV processes to degrade  
86 the RBCMs which exist in the H<sub>2</sub>SO<sub>4</sub> leachate during P extraction in our previous study.<sup>[3]</sup> The  
87 high RBCMs-containing solution was subjected for several tests to evaluate the effectiveness  
88 of their removal/degradation. The role of reaction time and initial concentrations of Fe<sup>2+</sup> and  
89 H<sub>2</sub>O<sub>2</sub> to influence the RBCMs degradation was evaluated. Furthermore, changes on structure  
90 and molecular weight of the RBCMs in the P-extraction solution were investigated by HPLC  
91 (high performance liquid chromatography) and UV-via spectroscopic analysis, which provided  
92 have given the insight into of the reactions.

93

## 94 **Materials and Methods**

95

### 96 ***Materials***

97 The High RBCMs-containing solution studied was the leachate from P-saturated alum sludge,  
98 which was used as substrate in laboratory scale engineered wetland for an animal farm  
99 wastewater treatment. The leachate/solution was obtained during P desorption study by using  
100 H<sub>2</sub>SO<sub>4</sub> leaching at a dose of 0.063 M.<sup>[3]</sup> By using inductively coupled plasma-mass  
101 spectrometry (ICP-MS), Hach spectrophotometer (DR/2800) and pH meter (ATI ORION,  
102 model 720A), the sample solution was characterized and the results were listed in Table 1.  
103 Analytical grade hydrogen peroxide solution (30 %, w/w) and ferrous chloride tetrahydrate  
104 (FeCl<sub>2</sub>·4H<sub>2</sub>O) were used and they were purchased from Riedel-deHaën Chemical as received.

105 [Table 1 here]

### 106 ***Experimental procedure***

107 The experiments were carried out in a room temperature. A batch of 100 ml samples was put  
108 into a series of 250 ml flask added with different volume (0.5-10 ml) of hydrogen peroxide  
109 (H<sub>2</sub>O<sub>2</sub>) or different quantity of Fenton reagents. Thereafter, the flasks were placed on an orbital  
110 shaker (SSL1, Bibby Sterilin LTD, UK) at 220 rpm for a certain period shaking. Meanwhile,  
111 samples were taken from the flask at some specific shaking time for colour measurement

112 Photodegradation tests were conducted in a Pyrex glass beaker of 250 ml capacity, as shown  
113 in Fig.1. The reaction mixture inside the beaker, consisting of 100 ml sample solution and the  
114 precise amount of Fenton reagent, was continuously stirred with a magnetic bar. The sample  
115 solution was illuminated with a shortwave ultraviolet lamp (Model R-52G, UVP, USA), which  
116 is a highly uniform 254 nm UV source with high-intensity of 1.25 mW/cm<sup>2</sup> at 6 inches with the  
117 filter. The beam was parallel and the length between lamp and surface of the solution was kept  
118 12 cm. The lamp was warmed up for 10 minutes to reach constant output. Samples were taken  
119 at a regular time interval to determine the color removal.

120 Pre-test has shown an insignificant change of pH (in order of 0.1–0.3 units) during the  
121 reaction process. Therefore there was no pH re-adjustment during the experiments reported.

122 All the experiments were repeated twice or three times and the results were shown in  
123 average value.

124 [Figure 1 here]

### 125 *Analytical techniques*

126 Measurements of colour were performed as per standard method using the HACH  
127 spectrophotometer (model DR-2800) according to standard method. H<sub>2</sub>O<sub>2</sub> residual was roughly  
128 monitored by Merckhoquant peroxide test strips (0.5–25 mg/L). In order to monitor the  
129 mineralization of RBCMs, measurements of TOC (100–700 mg/L) of sample solution, were  
130 conducted using the same HACH DR-2800 spectrophotometer following the sample digestion  
131 at 105 °C for 2 hours in a HACH DRB200 digester.

132 UV-vis spectroscopic measurements of the samples were performed on a Unicam heliosα  
133 UV-vis Spectrophotometer using 1 cm quartz cells. Specific UV absorbance at 254 nm, 280 nm  
134 and 400 nm (defined as UV<sub>254</sub>, UV<sub>280</sub> and Color<sub>400</sub>) were used to represent the concentrations  
135 of TOC, the normalized aromatic moieties and the color of the solution, respectively. To obtain  
136 more insight into the nature of RBCMs before and after treatment, the change of molecular size  
137 of RBCMs was measured by HPLC. The system consists of a Waters 1515 isocratic pump, a  
138 Waters 2487 UV dual λ detector operated at 254 nm, A PL Aquagel-OH 40 (300×7.5 mm)  
139 column. The mobile phase is 20 mM phosphate buffer solution (1.36g/L KH<sub>2</sub>PO<sub>4</sub>, 3.58 g/L  
140 Na<sub>2</sub>HPO<sub>4</sub>, pH=6.85). The eluent flow rate was 1.3 mL/min. 10 μL samples were injected into  
141 the system manually

142

### 143 **Results**

144

145 ***RBCMs degradation by different systems***

146 *H<sub>2</sub>O<sub>2</sub> oxidation*

147 Fig. 2 shows the RBCMs degradation in the form of colour removal of sample with reaction  
148 time at different H<sub>2</sub>O<sub>2</sub> concentrations. It can be seen from Fig. 2 that, during its initial stage,  
149 the percentage decrease of color rapidly increased with increasing initial H<sub>2</sub>O<sub>2</sub> concentration. It  
150 was observed that after one hour, the colour removal by 0.05, 0.10, 0.19, 0.38, 0.55, 0.73 and  
151 0.89 M H<sub>2</sub>O<sub>2</sub> was 5.9 %, 9.0 %, 10.1 %, 24.2 %, 29.5 %, 36.8 % and 38.2 %, respectively. But  
152 after 24 hours, there is no significant difference of color removal efficiencies with various  
153 H<sub>2</sub>O<sub>2</sub> concentrations tested. After 72 hours, over 99 % color removal was achieved regardless  
154 of the H<sub>2</sub>O<sub>2</sub> concentrations adopted. Obviously, during the first 8 hours, the increase of the  
155 initial H<sub>2</sub>O<sub>2</sub> concentration was mainly due to speed up the reaction. After ample reaction time  
156 and also at the end of the reaction, nearly all the color has been removed/degraded and thus the  
157 reactions under different H<sub>2</sub>O<sub>2</sub> concentrations become the same. In view of using fewer  
158 reagents, the H<sub>2</sub>O<sub>2</sub> concentration of 0.05 M and 0.10 M were adopted in subsequent  
159 experiments.

160 [Figure 2 here]

161  
162 Residual H<sub>2</sub>O<sub>2</sub> and TOC removals at different initial H<sub>2</sub>O<sub>2</sub> concentrations were measured at  
163 24 hours, 48 hours and 72 hours, respectively, and the results were showed in Table 2. It can be  
164 seen that when initial concentration is 0.05 M, H<sub>2</sub>O<sub>2</sub> was fully consumed after 72 hours,  
165 corresponding TOC removal was found 58.8 %. This indicates a significant  
166 removal/degradation of RBCMs which have been mineralized to CO<sub>2</sub> and H<sub>2</sub>O. As compared  
167 with the case of 0.05 M H<sub>2</sub>O<sub>2</sub> used, when H<sub>2</sub>O<sub>2</sub> initial concentration is 0.10 M, there was still  
168 around 0.74 mM H<sub>2</sub>O<sub>2</sub> left in the system after 72 hours. However, the TOC remains the same  
169 level of removal under the two H<sub>2</sub>O<sub>2</sub> concentrations.

170 [Table 2 here]

171

172 *Fenton treatment*

173 The results of the Fenton treatment for colour removal with and without stirring were  
174 illustrated in Fig. 3. The dosage of Fenton reagent was 0.5 mM for Fe<sup>2+</sup> and 0.05 or 0.1 M for  
175 H<sub>2</sub>O<sub>2</sub> in 100 ml sample. As shown in Fig. 3, there is little difference between stirring (at 220  
176 rpm) and non-stirring during the Fenton reaction regarding the colour removal. There is also no  
177 obvious trend of colour removal with the H<sub>2</sub>O<sub>2</sub> dosage between 0.05 M and 0.1 M. However, it  
178 is evident that the colour removal was enhanced with Fenton reaction time especially in the  
179 first 8 hours of test. The colour removal efficiency remains insignificant change after 24 hours  
180 of reaction, at that time and it was noted that over 95 % of colour was removed during this  
181 period. It should be noted that a negative removal of colour, as shown in Fig. 3, was appeared  
182 in the first hour of reaction since Fe<sup>2+</sup> was oxidized by H<sub>2</sub>O<sub>2</sub> to Fe<sup>3+</sup> which exhibited  
183 brown/yellow colour at the beginning of reaction.

184 [Figure 3 here]

185

186 Table 3 provides the results of Fenton treatment on TOC removal. It is very interesting to  
187 point out that although there is no obvious difference on colour removal between stirring and  
188 non-stirring, stirring clearly benefits the TOC removals. As shown in Table 3, stirring can  
189 enhance the speed of H<sub>2</sub>O<sub>2</sub> exhaustion and therefore it leads to additional 8 % (on average)  
190 TOC removals from 24 hours to 72 hours reaction. In particular, this has been highlighted in  
191 the case of initial H<sub>2</sub>O<sub>2</sub> of 0.1 M being adopted. RBCMs degradation by Fenton reaction can be  
192 simply described by equation 1.



194 It is clear that the part of the RBCMs can be mineralized to CO<sub>2</sub> and H<sub>2</sub>O. Stirring is therefore  
195 beneficial for continuous reaction by blowing CO<sub>2</sub> from the solution, leading to higher TOC  
196 (RBCMs) removal. Thus, stirring was adopted in the ensuing experiments

197 [Table 3 here]

198

199 To further clarify the influence of H<sub>2</sub>O<sub>2</sub> and Fe<sup>2+</sup> dosages on RBCMs degradation, Fig. 4 and  
200 Table 4 provides the results of Fenton treatment with two levels of H<sub>2</sub>O<sub>2</sub> and three levels of  
201 Fe<sup>2+</sup> dosages. As expected, the color removal increased with increasing concentration of Fe<sup>2+</sup>,  
202 as shown in Fig. 4. This can be explained by the production of hydroxyl radical (HO•) related  
203 to Fe<sup>2+</sup> concentration. When the initial concentration of Fe<sup>2+</sup> is less than 0.5 mM, the  
204 production rate of hydroxyl radical has a linear relation with Fe<sup>2+</sup> in the first stage of Fenton  
205 process.<sup>[22]</sup> This can also be confirmed by the decrease of H<sub>2</sub>O<sub>2</sub> which is showed in Table 4.  
206 Higher Fe<sup>2+</sup> concentration will accelerate H<sub>2</sub>O<sub>2</sub> to produce HO•. Interestingly, it is noted from  
207 Fig. 4 that, when the Fe<sup>2+</sup> concentrations remain the same levels, addition of H<sub>2</sub>O<sub>2</sub> of 0.1 M  
208 shows the less color removal efficiency than that of 0.05 M within 8 hours. This would be due  
209 to self-decomposition of H<sub>2</sub>O<sub>2</sub> to O<sub>2</sub> and H<sub>2</sub>O, and the recombination of HO• radicals.<sup>[23]</sup>  
210 However, it can be seen from Fig. 4 that, after 24 hours reaction, both 0.05 M and 0.1 M H<sub>2</sub>O<sub>2</sub>  
211 showed similar ability for colour removal. It should be pointed out that during the final stage of  
212 the Fenton reaction, higher Fe<sup>2+</sup> would have a negative effect on color removal. It may be  
213 derived from the oxidation of residual Fe<sup>2+</sup> to Fe<sup>3+</sup> which exhibited yellow in color in the  
214 solution.

215 [Figure 4 here]

216 [Table 4 here]

217

218 In regard to TOC removal, it has increased with increasing reaction time but higher  $\text{Fe}^{2+}$   
219 seems to have adverse influence on TOC removal especially in longer time reactions, as shown  
220 in Table 4. The maximum TOC removal of 67.0 % was achieved at 72 hours by addition of 0.1  
221 M  $\text{H}_2\text{O}_2$  and 0.125 mM  $\text{Fe}^{2+}$ . On such condition, the color was fully eliminated.

#### 222 *Photo-Fenton treatment*

223 Fig. 5 and Table 5 show the results of colour and TOC removal during photo-Fenton process.  
224 The blank, i.e. the only UV irradiation, was conducted, which indicates that there is no use for  
225 enhancing color removal under the current UV lamp. Comparing the results with those shown  
226 in Fig. 4, the similar trends were observed. However, it is obviously noted that the photo-  
227 Fenton treatment significantly improves the color removal. After 8 hours UV irradiation,  
228 98.0 % color and 47.2 % TOC were removed by addition of 0.05 M  $\text{H}_2\text{O}_2$  and 0.5 mM  $\text{Fe}^{2+}$ .

229 [Figure 5 here]

230 [Table 5 here]

231

#### 232 *UV-vis spectroscopic analysis*

233 The UV-vis absorption spectra provide a useful tool to identify the change of structural  
234 characteristics and molecular weight of RBCMs. Such investigations of the selected samples  
235 before and after the different treatment processes were carried out and the results jointly  
236 illustrated in Fig. 6. The three treated samples (S1-S3) were collected from each of the  
237 following treatment processes at the optimal testing conditions which indicate in the legend of  
238 Fig. 6:  $\text{H}_2\text{O}_2$  oxidation (S1), Fenton reaction (S2) and photo-Fenton treatment (S3). It is well  
239 known that the UV-vis spectra of RBCMs are broad, featureless and monotonously decrease  
240 with increasing wavelength. For the original sample (S0), it has a high absorbance between  
241 200–330 nm. After 330 nm, the absorbance decreases sharply with increasing wavelength, as  
242 shown in Fig. 6. Notably, compared with S0, the significant decrease of absorbencies of S1, S2

243 and S3 after treatments can be observed in Fig. 6. It should be pointed out that the S3 was  
244 tested at a high  $\text{Fe}^{2+}$  concentration with short reaction time, this may cause the S3 curve being  
245 above the S1 and S2 in Fig. 6 since the UV illuminating can promote to produce a great deal of  
246  $\text{Fe}^{3+}$  which has a similar absorbency characteristics with RBCMs in 200–400 nm regions, thus  
247 resulting in a negative effect of the UV-vis absorption spectra. As per literature, various  
248 absorption at wavelengths of 250, 254, 270, 280, 300, 365, 400, 436 and 465 nm as well as  
249 ratios like  $\text{Abs}_{250}/\text{Abs}_{365}$ ,  $\text{Abs}_{465}/\text{Abs}_{665}$  have been cited for the spectral differentiation of  
250 NOM.<sup>[24]</sup> Among them, absorbencies at 254 nm ( $\text{UV}_{254}$ ) and 400 nm ( $\text{Color}_{400}$ ) were  
251 interchangeably measured with TOC and colour, respectively.<sup>[6,25,26]</sup> The range of 260–290 nm  
252 indicates the occurrence of  $\pi$ - $\pi^*$  electron transitions for phenolic substances, aniline derivatives,  
253 benzoic acids, polyenes and polycyclic aromatic hydrocarbons.<sup>[27]</sup> Moreover, since many of  
254 these substances are precursors or components of certain types of NOM, the value of  
255 absorptivity at 280 nm ( $\text{UV}_{280}$ ) may yield important clues regarding the degree of aromaticity,  
256 source functions, extent of humification and possible molecular weight.<sup>[28]</sup> Thus, similarly in  
257 this study, absorptivity at 280 nm is specially viewed as an indication of the structural feature  
258 of RBCMs. It can be seen from Fig. 6 that the shoulder in the range of 260–290 nm of S0  
259 disappeared as a result of the treatments especially in  $\text{H}_2\text{O}_2$  oxidation and Fenton process.  
260 These results suggest that some unsaturated components, such as aromatic moieties in the  
261 RBCMs, may well be degraded during these treatments.

262 The attached diagram within Fig. 6 is the plot of  $\Delta\log K$  corresponding to S0, S1, S2 and S3.  
263 The  $\Delta\log K$  is a major parameter, which is increased with the molecular size of NOM and free  
264 radical concentration.<sup>[29]</sup> The value of  $\Delta\log K$  can be calculated by subtracting the logarithm of  
265 the absorptivity at 600 nm from that at 400 nm. As shown in Fig. 6, the obvious decreases in  
266  $\Delta\log K$  values of all treated samples especially for S2 were observed, providing hard evidence  
267 of the fact that some RBCMs were broken down into smaller molecules after these treatments.

268 As a visible appearance, Fig. 7 shows the original and treated samples marked as S0, S1, S2  
269 and S3 with previous denotation.

270 [Figure 6 here]

271 [Figure 7 here]

### 272 ***Result of HPLC measurement***

273 HPLC was employed to monitor the molecular size of the RBCMs before and after the  
274 treatment based on the principle of size-exclusion. It is understood that the large molecular size  
275 will be detected first followed by the small molecular size of the RBCMs. Similarly, big  
276 peak/absorbance indicates the strong amount of RBCMs and small peak refers to the light  
277 amount of the RBCMs. From Fig. 8, it is seen clearly that the RBCMs before treatment (S0)  
278 possess heavy mass with big molecular size while the RBCMs after treatment (S2) exhibit  
279 small molecular size with low amount, indicating the breakdown of the RBCMs by Fenton  
280 reaction.

281 [Figure 8 here]

282

### 283 **Discussion**

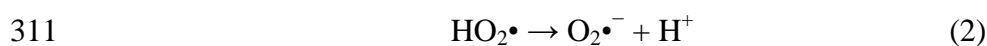
284

285 Although the degradation of NOM has been investigated extensively in the literature, it is  
286 noted that, NOM came from either some industrial products or isolated from special nature  
287 organic materials as per the investigations reported. Hence, the components of NOM are  
288 relatively simple and the concentrations are lower than the samples investigated in this study.  
289 As described earlier, the samples studied currently were derived from a novel study aimed at  
290 reusing the dewatered alum sludge cake as P adsorbent and biofilm carrier in constructed  
291 wetland for P-rich wastewater treatment.<sup>[2,3]</sup> After a long time operation in wetland of reuse,  
292 the alum sludge was finally saturated by P from the wastewater. In order to not only decrease

293 the risk of disposal of P-saturated alum sludge but also try to recovery P from it as a recycled  
294 resource, extraction by using H<sub>2</sub>SO<sub>4</sub> was proved to be an efficient and economic method for P  
295 release.<sup>[3]</sup> However, RBCMs and metals such as Al, Ca, Mg and Fe were also released into  
296 solution at the same time, forming a special sample with strong colour, low pH, high  
297 concentrations of P, Al, RBCMs and other components (see Table 1). Therefore, there is a  
298 necessity to remove colour and RBCMs from the H<sub>2</sub>SO<sub>4</sub> extracted solution during the attempt  
299 of obtaining the pure phosphate as final target in P recovery.

300 H<sub>2</sub>O<sub>2</sub> oxidation was tested firstly because the nature of H<sub>2</sub>O<sub>2</sub> is a strong (oxidation potential  
301 =1.78 V), but not very specific oxidizing agent. As a result, high yields of degradation products  
302 are expected. However, the results show that the reaction time is the key factor for colour and  
303 TOC removal. The reason behind is that most substances do not react rapidly with H<sub>2</sub>O<sub>2</sub> and, in  
304 order to achieve oxidation, activation of H<sub>2</sub>O<sub>2</sub>, such as transition metal, alkaline conditions, is  
305 required.<sup>[30]</sup> Whereas, H<sub>2</sub>O<sub>2</sub> oxidation was carried out in this study at very low pH  
306 (approximately 2). This may have caused the slow reaction and thus a long time reaction is  
307 necessary.

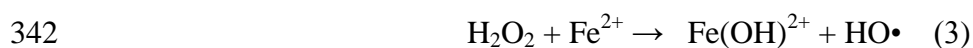
308 The Fenton reagent has been shown to be effective in the degradation of a wide spectrum of  
309 organic and inorganic pollutants.<sup>[31-33]</sup> More recently, Watts and Teel<sup>[34]</sup> reported an important  
310 reaction during Fenton process:

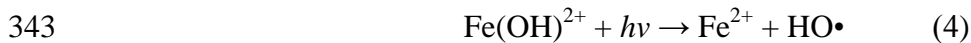


312 These propagation reactions produce a pool of radicals with different reactive properties.  
313 Hydroxyl radical (HO•) and perhydroxyl radical (HO<sub>2</sub>•) are both oxidant although the latter is  
314 relatively weak. Superoxide radical (O<sub>2</sub>•<sup>-</sup>) is a weak reductant and nucleophile in aqueous  
315 systems which may be responsible for an enhanced treatment of contaminants when they don't  
316 react with hydroxyl radicals.<sup>[34]</sup> As a result, Fenton treatment can be used widely for  
317 degradation of many kinds of pollutants.

318 Because  $\text{Fe}^{3+}$  ions exist mostly as hydroxyl complexes and soluble  $\text{Fe}^{2+}$  salts tend to co-  
319 precipitate with  $\text{Fe}^{3+}$  oxyhydroxides if ions are present at neutral pH, Fenton reaction is  
320 therefore most effective in acidic solution (pH~3) which keeps  $\text{Fe}^{3+}$  species soluble. [5] The pH  
321 of the samples in this study is around 2.1, thus it is suitable for Fenton reaction. As reported in  
322 Fig. 2 & 4 and Table 2 & 4, compared with  $\text{H}_2\text{O}_2$  oxidation, Fenton reaction can increase  
323 distinctly the rate of colour removal within initial 8 hours. The possible reason maybe lies in  
324 the enhanced mass of radicals including  $\text{HO}\cdot$ ,  $\text{HO}_2\cdot$  and  $\text{O}_2\cdot^-$  being produced and reacted  
325 quickly with some easily destroyed chromophores of RBCMs, such as aromatic ring in the first  
326 stage. However, the rate of radicals production becomes slow and the left components of  
327 RBCMs become difficult to be destroyed with increasing reaction time. Therefore, the overall  
328 colour and TOC removal efficiencies can't be improved significantly. It should be pointed out  
329 that, firstly, at low  $\text{H}_2\text{O}_2$  concentration of 0.5 M, the  $\text{H}_2\text{O}_2$  oxidation was slightly better than  
330 Fenton reaction for TOC removal (see Table 2, 4). The reason was assumed that, because of  
331 catalysis of  $\text{Fe}^{2+}$ , there are not only high oxidants of  $\text{H}_2\text{O}_2$  and  $\text{HO}\cdot$  but also weak oxidant of  
332  $\text{HO}_2\cdot$  and weak reductant of  $\text{O}_2\cdot^-$  in the reaction system. Thus, in low concentration of  $\text{H}_2\text{O}_2$ ,  
333 the negative effect of  $\text{HO}_2\cdot$  and  $\text{O}_2\cdot^-$  is striking, leading to  $\text{H}_2\text{O}_2$  being slightly better than  
334 Fenton on total ability of oxidation. Secondly, the high concentration of  $\text{Fe}^{2+}$  brings a negative  
335 effect on TOC removal though it is positive for production rate of  $\text{HO}\cdot$  in first stage of Fenton  
336 process. The supposed reason is that the excessive  $\text{Fe}^{2+}$  can be adsorbed by RBCMs due to the  
337 capability of RBCMs to complex metal ions [35] to form complex which is more difficult to be  
338 broken down into  $\text{CO}_2$  and  $\text{H}_2\text{O}$  than RBCMs.

339 A combination of  $\text{H}_2\text{O}_2$  and UV irradiation with  $\text{Fe}^{2+}$ , a so-called photo-Fenton process, can  
340 significantly enhance the decomposition of many refractory organic compounds. The main  
341 mechanism of photo-Fenton process is as follows:





344 The acceleration for decomposition of organic compounds is believed to be in order to  
345 photolysis of iron aquacomplex,  $\text{Fe(H}_2\text{O)}_5(\text{OH})^{2+}$  (respected hereafter by  $\text{Fe(OH)}^{2+}$ ), to  
346 providing a new important source of  $\text{HO}\cdot$  radicals.<sup>[36,37]</sup> It is also confirmed from the results of  
347 this study that photo-Fenton showed the highest efficiency for colour removal. After 8 hours  
348 irradiation, 97.8 % colour was removed whereas only 54.7 % and 81.1 % colour were removed  
349 by  $\text{H}_2\text{O}_2$  and Fenton processes, respectively, at the same reaction period of 8 hours. In addition,  
350 the high TOC removal of 47.2 % was also achieved in the same time.

351 Comparing the three processes tested in the current study, they are all based on the  $\text{H}_2\text{O}_2$   
352 oxidation actually. UV and  $\text{Fe}^{2+}$  act as the activator for improving the oxidation ability of  $\text{H}_2\text{O}_2$ .  
353 As per the results and the discussion, the photo-Fenton system showed the highest ability on  
354 colour and TOC removals. But considering the investment and danger of UV irradiation for  
355 operator, UV-assisted systems may not be the convenient and economical choice. Compared  
356 with  $\text{H}_2\text{O}_2$  oxidation, Fenton system can increase TOC removal from 58.6 % to 67.0 % but a  
357 small quantity of ferrous salts addition is required. However, the main advantage of  $\text{H}_2\text{O}_2$   
358 oxidation is that it doesn't bring any additional compound to the system.

359

## 360 **Conclusions**

361

362 The  $\text{H}_2\text{SO}_4$  leachate samples, consisting of a large amount of RBCMs, phosphate and  
363 aluminium, were treated by  $\text{H}_2\text{O}_2$ , Fenton and photo-Fenton systems, respectively, for the  
364 purpose of degradation of RBCMs in regard to colour and TOC. The results of colour and TOC  
365 removals showed that all of the three processes are efficient. Among them, photo-Fenton is the  
366 most efficient process because around 98 % colour and 47 % TOC were removed after 8 hours  
367 reaction. For  $\text{H}_2\text{O}_2$  and Fenton systems, the reaction rate is comparatively slow and the reaction

368 time is the key factor for colour and TOC removals although 100 % colour and 58.6 % TOC  
369 could disappear by using H<sub>2</sub>O<sub>2</sub> while 100% colour and 67.0 % TOC could be eliminated by  
370 using Fenton oxidation, both in 72 hours of reaction. It was found that higher concentration of  
371 H<sub>2</sub>O<sub>2</sub> (0.1 M) is favourable than that of 0.05 M for colour removal. However, excessive Fe<sup>2+</sup>  
372 brings a negative effect on TOC removal. Bearing in mind of the main objective of this study,  
373 it lies in seeking a RBCMs reduction approach which is efficient and easy to operate in practice.  
374 Therefore, considering the investment and danger of UV irradiation, H<sub>2</sub>O<sub>2</sub> and Fenton system  
375 could be suitable methods for practical operation.

376

### 377 **Acknowledgements**

378

379 The authors wish to acknowledge the research funding provided by the Environmental  
380 Protection Agency, Ireland through the Environmental Technologies Scheme (project no.  
381 2005-ET-MS-38-M3). The first author would like to thank University College Dublin for the  
382 *Ad Astra* scholarship. Mr. Patrick Kearney, Section head technician, Water and Effluents  
383 Laboratory, UCD, is also thanked for his invaluable assistance.

384

### 385 **References**

386

- 387 [1] Zhao, Y.Q.; Babatunde, A.O.; Zhao, X.H.; Li, W.C. Development of alum sludge-based  
388 constructed wetland: An innovative and cost-effective system for wastewater treatment. *J.*  
389 *Environ. Sci. Health Pt. A* **2009**, *44*(8), 827-832.
- 390 [2] Zhao, Y.Q.; Zhao, X.H.; Babatunde, A.O. Use of dewatered alum sludge as main substrate  
391 in treatment reed bed receiving agricultural wastewater: Long-term trial. *Bioresource*  
392 *Technol.* **2009**, *100*, 644-648.

- 393 [3] Zhao, X.H.; Zhao, Y.Q. Investigation of phosphorus desorption from P-saturated alum  
394 sludge used as a substrate in constructed wetland. *Sep. Purif. Technol.* **2009**, *66*, 71-75.
- 395 [4] Paciolla, M.D.; Kolla, S.; Jansen, S.A. The reduction of dissolved iron species by humic  
396 acid and subsequent production of reactive oxygen species. *Adv. Environ. Res.* **2002**, *7*,  
397 169-178.
- 398 [5] Lipczynska-Kochany, E.; Kochany, J. Effect of humic substances on the Fenton treatment  
399 of wastewater at acidic and neutral pH. *Chemosphere*, **2008**, *73*, 745-750.
- 400 [6] Liao, C.-H.; Lu, M.-C.; Su, S.-H. Role of cupric ions in the H<sub>2</sub>O<sub>2</sub>/UV oxidation of humic  
401 acids. *Chemosphere*, **2001**, *44*, 913-919.
- 402 [7] Crozes, G.; White, P.; Marshall, M. Enhanced coagulation: its effect on NOM removal  
403 and chemical costs. *J. Am. Water Works Assoc.* **1995**, *87*, 79-89.
- 404 [8] Jacangelo, J.G.; Chellam, S.; Bonacquisti, T.P. Treatment of surface water by double  
405 membrane systems: assessment of fouling, permeate water quality and costs. *Water Sup.*  
406 **2000**, *18*, 438-441.
- 407 [9] Rodri'guez, E.; Encinas, A.; Masa, F. J.; Beltra'n, F. J. Influence of resorcinol chemical  
408 oxidation on the removal of resulting organic carbon by activated carbon adsorption.  
409 *Chemosphere*, **2008**, *70*, 1366-1374.
- 410 [10] Voelker, B.; Sulzberger, B. Effects of Fulvic Acid on Fe(II) Oxidation by Hydrogen  
411 Peroxide. *Environ. Sci. Technol.* **1996**, *30*, 1106-1114.
- 412 [11] Michelee, L.; Matthewa, T. Inhibition of Hydroxyl Radical Reaction with Aromatics by  
413 Dissolved Natural Organic Matter. *Environ. Sci. Technol.* **2000**, *34*, 444-449.
- 414 [12] Murray, C.A.; Parsons, S.A. Comparison of AOPs for the removal of natural organic  
415 matter: performance and economic assessment. *Water Sci. Technol.* **2004**, *49*, 267-272.
- 416 [13] Southworth, B.A.; Voelker, B. M. Hydroxyl Radical Production via the Photo-Fenton  
417 Reaction in the Presence of Fulvic Acid. *Environ. Sci. Technol.* **2003**, *37*, 1130-1136.

- 418 [14] Benitez, F.J.; Acero, J.L.; Real, F.J. Degradation of carbofuran by using ozone, UV  
419 radiation and advanced oxidation processes. *J. Hazard. Mater.* **2002**, *89*, 51-65.
- 420 [15] Cho, S.P.; Hong, S.C.; Hong, S. Photocatalytic degradation of the landfill leachate  
421 containing refractory matters and nitrogen compounds. *Appl. Catal. B: Environ.* **2002**, *39*,  
422 125-133.
- 423 [16] Andreozzi, R.; Caprio, V.; Insola, A.; Marotta, R. Advanced oxidation processes for  
424 water purification and recovery. *Catal. Today*, **1999**, *53*, 51-59.
- 425 [17] Nienow, A.M.; Bezares-Cruz, J. C.; Poyer, I. C.; Hua, I.; Jafvert, C.T. Advanced  
426 oxidation processes for water purification and recovery. *Chemosphere*, **2008**, *72*, 1700-  
427 1705.
- 428 [18] Wang, K.; Guo, J.; Yang, M.; Junji, H.; Deng, R. Decomposition of two haloacetic acids  
429 in water using UV radiation, ozone and advanced oxidation processes. *J. Hazard. Mater.*  
430 **2009**, *162*, 1243-1248.
- 431 [19] Ou, X.; Quan, X.; Chen, S.; Zhao, H.; Zhang, Y. Atrazine Photodegradation in Aqueous  
432 Solution Induced by Interaction of Humic Acids and Iron: Photoformation of Iron(II) and  
433 Hydrogen Peroxide. *J. Agric. Food Chem.* **2007**, *55*, 8650-8656.
- 434 [20] Murray, C.A.; Parsons, S. A. Removal of NOM from drinking water: Fenton's and photo-  
435 Fenton's processes. *Chemosphere*, **2004**, *54*, 1017-1023.
- 436 [21] Kitis, M.; Kaplan, S.S. Advanced oxidation of natural organic matter using hydrogen  
437 peroxide and iron-coated pumice particles. *Chemosphere*, **2007**, *68*, 1846-1853
- 438 [22] Gao, Y.; Zhang, Y.; Yang, M.; Hu, J. Comparison of Hydroxyl Radical Production Rates  
439 in H<sub>2</sub>O<sub>2</sub> Solution under Homogeneous Catalysis of Fe<sup>3+</sup> or Fe<sup>2+</sup>. *Environ. Sci.* **2006**, *27*,  
440 305-309.
- 441 [23] Buxton, G.V.; Greenstock, C.L.; Helman, W.P.; Ross, A.B. Critical review of rate  
442 constants for reaction of hydrated electrons, hydrogen atoms and hydroxyl radicals

- 443 (OH/•O<sup>-</sup>) in aqueous solution. *J. Phys. Chem. Ref. Dat.* **1988**, *17*, 513-518.
- 444 [24] Uyguner, C.S.; Bekbolet, M. Evaluation of humic acid photocatalytic degradation by  
445 UV-vis and fluorescence spectroscopy. *Catal. Today*, **2005**, *101*, 267-274.
- 446 [25] Katsumata, H; Sada, M.; Kaneco, S.; Suzuki, T.; Ohta, K.; Yobiko, Y. Humic acid  
447 degradation in aqueous solution by the photo-Fenton process. *Chem. Eng. J.* **2008**, *137*,  
448 225-230.
- 449 [26] Lim, S.M.; Chiang, K.; Amal, R.; Fabris, R.; Chow, C.; Drikas, M. A Study on the  
450 Removal of Humic Acid Using Advanced Oxidation Processes. *Sep. Sci. Technol.* **2007**,  
451 *42*,1391-1404.
- 452 [27] Traina, S.J.; Novak, J.; Smeck, N.E. An ultraviolet absorbance method of estimating the  
453 percent aromatic carbon content of humic acids. *J. Environ. Qual.* **1990**, *19*, 151-153.
- 454 [28] Chin, Y.-P.; Aiken, G.; O'Loughlin, E. Molecular-weight, Polydispersity, and  
455 Spectroscopic properties of aquatic humic substances. *Environ. Sci. Technol.* **1994**, *28*,  
456 1853-1858.
- 457 [29] Fukushima, M.; Tarsumi, K.; Nagao, S. Degradation Characteristics of Humic Acid  
458 during Photo-Fenton Processes. *Environ. Sci. Technol.* **2001**, *35*, 3683-3690.
- 459 [30] Allard, B.; Derenne, S. Oxidation of humic acids from an agricultural soil and a lignite  
460 deposit: Analysis of lipophilic and hydrophilic products. *Org. Geochem.* **2007**, *38*, 2036-  
461 2057.
- 462 [31] Neyens, E.; Baeyens, J. Hydrogen peroxide photolysis in acidic aqueous solutions  
463 containing chloride ions. II. Quantum yield of OH radicals. *J. Hazard. Mater.* **2003**, *98*,  
464 33-50.
- 465 [32] Pignatello, J.J.; Oliveros, E.; MacKay, A. Advanced oxidation processes for organic  
466 contaminant destruction based on the Fenton reaction and related chemistry. *Crit. Rev.*  
467 *Environ. Sci. Technol.* **2006**, *36*, 1-84.

- 468 [33] Georgi, A.; Schierz, A.; Trommler, U.; Horwitz, C.P.; Collins, T.J.; Kopinke, F.-D.  
469 Humic acid modified Fenton reagent for enhancement of the working pH range. *App.*  
470 *Catal. B-Environ.* **2007**, *72*, 26-36.
- 471 [34] Watts, R.J.; Teel, A.M. Chemistry of modified Fenton's reagent (catalyzed H<sub>2</sub>O<sub>2</sub>  
472 propagations-CHP) for in situ soil and groundwater remediation. *J. Environ. Eng. ASCE*  
473 **2005**, *131*, 612-622.
- 474 [35] Alvarez-Puebla, R.A.; Valenzuela-Calahorro, C.; Garrido, J.J. Cu(II) retention on a humic  
475 substance. *J. Colloid Interf. Sci.* **2004**, *270*, 47-55.
- 476 [36] Brand, N.; Mailhot, G.; Bolte, M. Degradation photoinduced by Fe(III): method of  
477 alkylphenol ethoxylates removal in water. *Environ. Sci. Technol.* **1998**, *32*, 2715-2720.
- 478 [37] Mailhot, G.; Astruc, M.; Bolte, M. Degradation of tributyltin chloride in water  
479 photoinduced by iron(III). *Appl. Organometal. Chem.* **1998**, *13*, 53-61.
- 480  
481  
482  
483  
484  
485  
486  
487  
488  
489  
490  
491  
492

493

Table 1 The characteristics of the sample (P-extraction leachate)

pH	Color (Pt-Co units)	Chemical oxygen demand (COD) (mg/L)	Total organic carbon (TOC) (mg/L)	Phosphorus (as PO <sub>4</sub> <sup>3-</sup> ) (mg/L)	Aluminum (Al) (mg/L)	Calcium (Ca) (mg/L)	Magnesium (Mg) (mg/L)	Iron (Fe) (mg/L)
~2.1	4100	1026	430	720.6	346.4	74.8	10.88	8.98

494

495

496

497

498

499

500

501

502

503

504

505

506

507

508

509

510

511

512

513

Table 2: H<sub>2</sub>O<sub>2</sub> residual and TOC removal at different H<sub>2</sub>O<sub>2</sub> concentrations

H <sub>2</sub> O <sub>2</sub>	Residual H <sub>2</sub> O <sub>2</sub> (mM)			TOC removal (%)		
	24 hrs	48 hrs	72 hrs	24 hrs	48 hrs	72 hrs
0.05 M	> 0.74	> 0.74	0	45.58	52.79	58.84
0.1 M	> 0.74	> 0.74	0.74	38.37	48.79	58.60

514

515

516

517

518

519

520

521

522

523

524

525

526

527

528

529

530

531

532

533

534

Table 3: Results of H<sub>2</sub>O<sub>2</sub> residual and TOC removal during Fenton reagent treatment

	Residual H <sub>2</sub> O <sub>2</sub> (mM)			TOC removal (%)		
	24 hrs	48 hrs	72 hrs	24 hrs	48 hrs	72 hrs
0.05 M H <sub>2</sub> O <sub>2</sub> (NS)	0.15–0.29	0.15	0	38.84	41.40	44.56
0.05 M H <sub>2</sub> O <sub>2</sub> (S)	0	0	0	49.30	49.77	51.40
0.10 M H <sub>2</sub> O <sub>2</sub> (NS)	> 0.74	0.29–0.74	0	43.49	50.47	58.03
0.10 M H <sub>2</sub> O <sub>2</sub> (S)	> 0.74	0	0	57.67	62.56	64.42

Note: CFe<sup>2+</sup> = 0.5 mM; NS: non stirring; S: stirring (at 220 rpm)

535

536

537

538

539

540

541

542

543

544

545

546

547

548

549

550

551

552

553

Table 4 Residual H<sub>2</sub>O<sub>2</sub> and TOC removal using different H<sub>2</sub>O<sub>2</sub> and Fe<sup>2+</sup> dosages

H <sub>2</sub> O <sub>2</sub> (M)	Fe <sup>2+</sup> (mM)	Residual H <sub>2</sub> O <sub>2</sub> (mM)			TOC removal (%)		
		24 hrs	48 hrs	72 hrs	24 hrs	48 hrs	72 hrs
	0.500	0	0	0	49.30	49.77	51.40
0.05	0.250	0.06	0	0	51.16	53.72	54.74
	0.125	> 0.74	0	0	46.28	53.95	54.88
	0.500	> 0.74	0	0	57.67	62.56	64.42
0.10	0.250	> 0.74	> 0.74	0	47.67	65.39	66.28
	0.125	> 0.74	> 0.74	0.15–0.29	40.47	57.44	66.98

554

555

556

557

558

559

560

561

562

563

564

565

566

567

568

569

570

571

572

Table 5: H<sub>2</sub>O<sub>2</sub> residual and TOC removal after 8 hrs photo-Fenton treatment

H <sub>2</sub> O <sub>2</sub> (M)	0.05			0.10		
Fe <sup>2+</sup> (mM)	0.500	0.250	0.125	0.500	0.250	0.125
Residual H <sub>2</sub> O <sub>2</sub> (mM)	0.15–0.29	0.74	> 0.74	> 0.74	> 0.74	> 0.74
TOC removal (%)	47.21	36.05	24.65	43.26	33.49	25.58

573

574

575

576

577

578

579

580

581

582

583

584

585

586

587

588

589

590

591

592

593 **Figure captions**

594

595 Fig. 1 Schematic diagram of the photo reactor

596 Fig. 2. The removal of color at different H<sub>2</sub>O<sub>2</sub> concentrations

597 Fig. 3. Results of color removal via Fenton treatment

598 Fig. 4. Effect of different H<sub>2</sub>O<sub>2</sub> and Fe<sup>2+</sup> dosages on color removal

599 Fig. 5. Colour removals during photo-Fenton process

600 Fig. 6. UV-vis absorption spectra and ΔlogK before and after the different treatments

601 Fig. 7. The visible observation of the samples before and after different treatments: S0, original

602 sample; S1, H<sub>2</sub>O<sub>2</sub> oxidation; S2, Fenton reaction; and S3, photo-Fenton treatment

603 Fig. 8. Results of RBCMs molecular size monitoring before and after Fenton reaction by HPLC

604

605

606

607

608

609

610

611

612

613

614

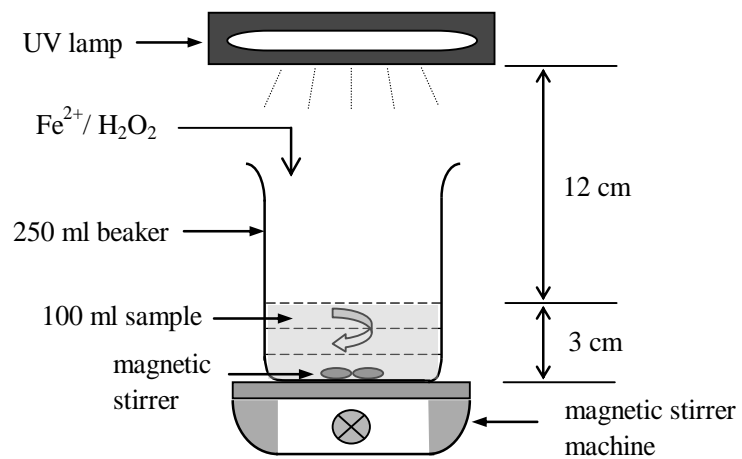
615

616

617

618 Figure 1

619



620

621

622

623

624

625

626

627

628

629

630

631

632

633

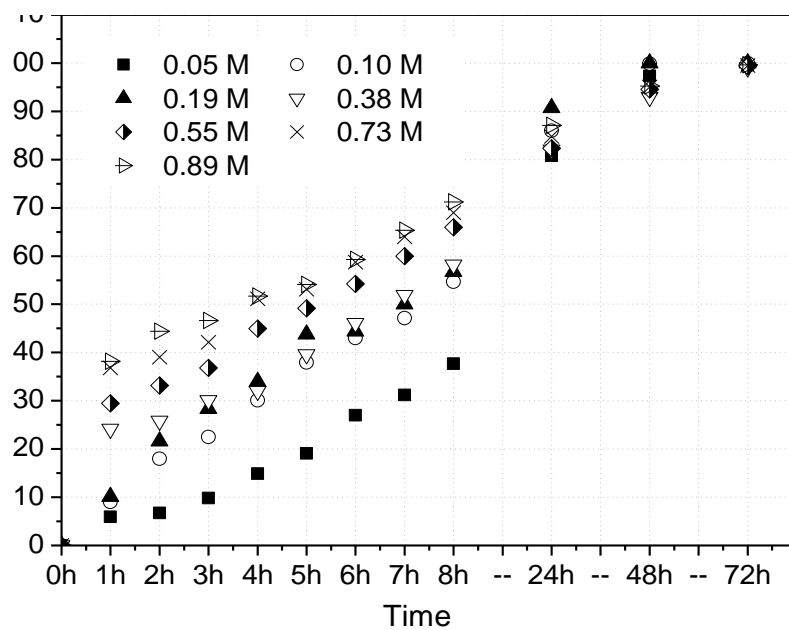
634

635

636

637 Figure 2

638



639

640

641

642

643

644

645

646

647

648

649

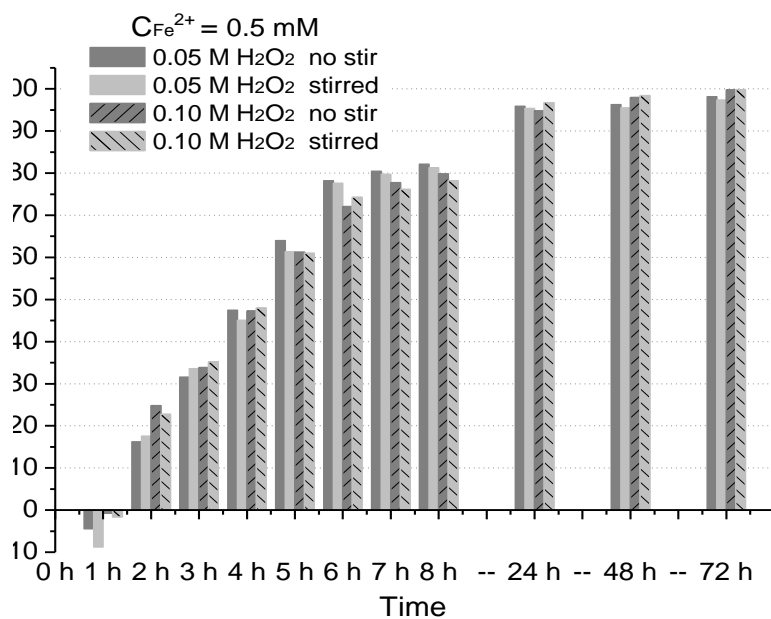
650

651

652

653 Figure 3

654



655

656

657

658

659

660

661

662

663

664

665

666

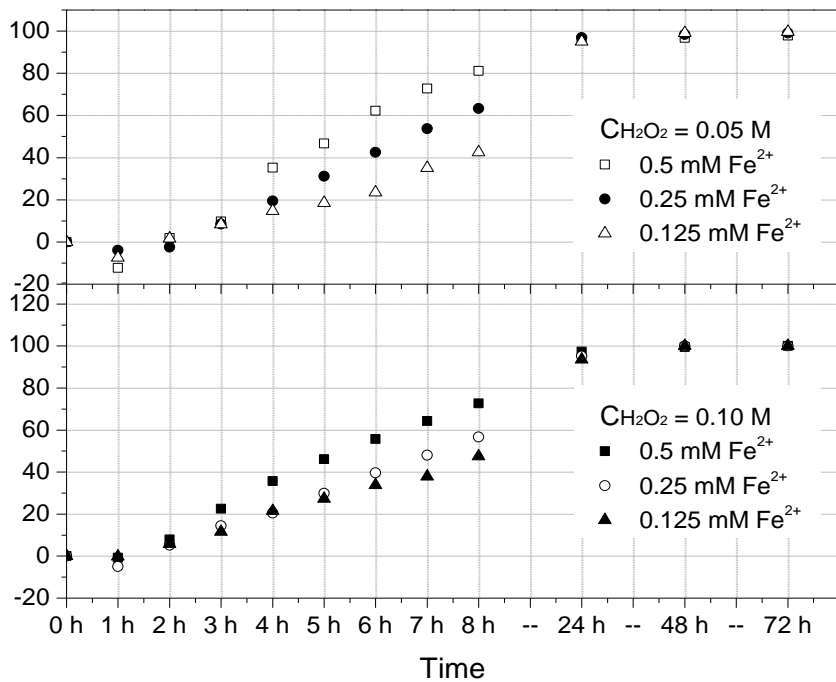
667

668

669

670 Figure 4

671



672

673

674

675

676

677

678

679

680

681

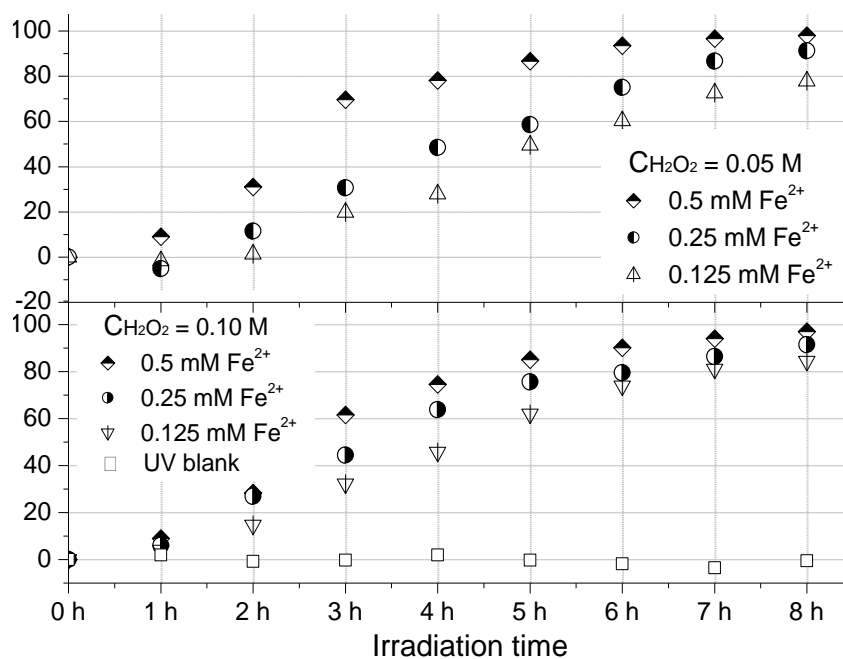
682

683

684

685 Figure 5

686



687

688

689

690

691

692

693

694

695

696

697

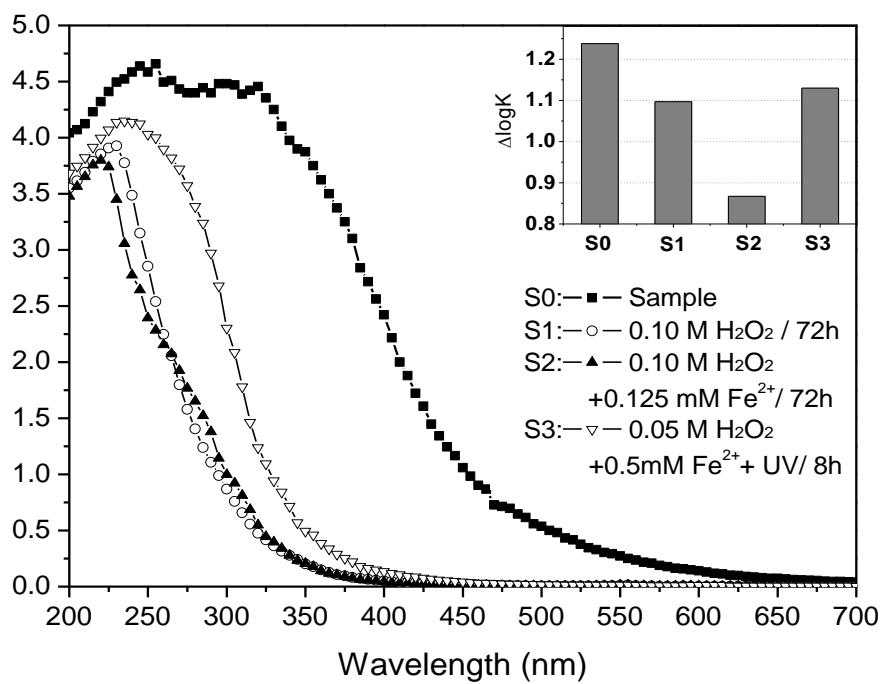
698

699

700

701 Figure 6

702



703

704

705

706

707

708

709

710

711

712

713

714

715

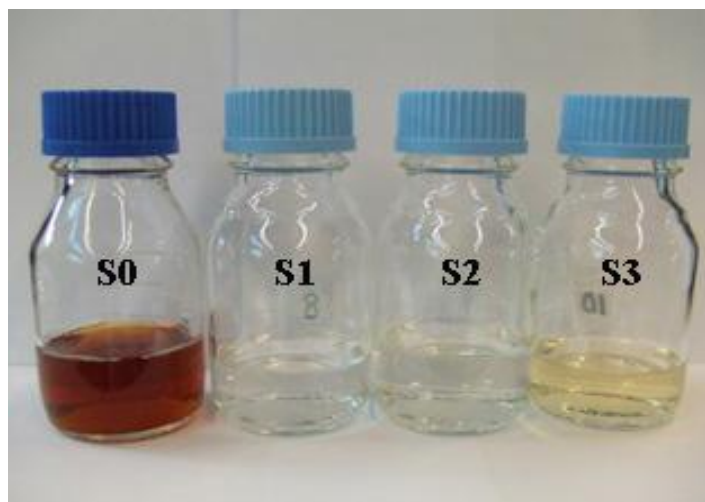
716

717 Figure 7

718

719

720



721

722

723

724

725

726

727

728

729

730

731

732

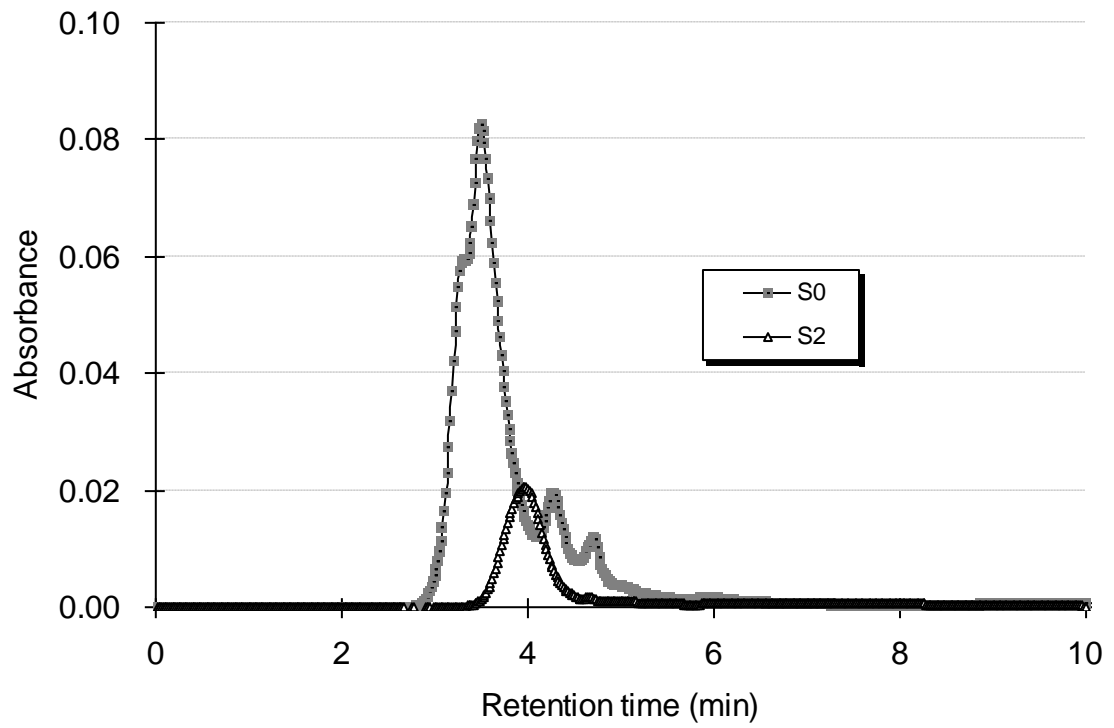
733

734

735

736 Figure 8

737



738

739

740

741

742

743

744

745

746

747

748

749